

# Fault System Delineation Driven by New Technology in Tazhong Karsted Carbonate Reservoirs

Xingliang DENG<sup>1</sup>, Yanming TONG<sup>2</sup>, Shiti CUI<sup>1</sup>, Chuan WU<sup>2</sup>, Chunguang SHEN<sup>1</sup>,  
Gaige WANG<sup>2</sup>, Jiangyong WU<sup>1</sup>, Pin YANG<sup>2</sup>, Chenqing TAN<sup>2</sup>, Aida Abdullah Abri<sup>3</sup>

<sup>1</sup>PetroChina Tarim Company, Korla, CHINA

<sup>2</sup>SLB, Beijing, CHINA

<sup>3</sup>SLB, Dhahran, Saudi Arabia

## EXTENDED ABSTRACT

The Tazhong paleo-uplift is one of the most important hydrocarbon enrichment areas in Tarim Basin, NW China. After years of exploration, many reservoirs have been discovered in the deep Paleozoic karsted carbonate rocks. Fault system plays a very important role in Tazhong area in terms of karsted carbonate reservoir development and enhancement, and even hydrocarbon accumulation. While detailed and robust fault system delineation is the biggest obstacle nowadays to predict reservoirs more accurately and in turn design optimized well placement. We solved this difficulty to a great extent by applying a series of new technologies and geological knowledge.

The first step was to improve the quality of seismic image. The technology of “vector high fidelity signal enhance” was used to enhance the natural bandwidth of seismic imaged volumes by simultaneously optimizing the signal and frequency content. Application of this technology improved temporal resolution, reduced noise, and extended usable bandwidth for structural interpretation. This technology was amplitude and phase features preservation process which could improve resolution for interpretation and pre-stack and post-stack seismic inversion and could provide additional structural details and correlated volumes useful for seismic volume attribute extraction. This technology processed the original amplitude volume with following operations: Radon filtering, i.e. Radon domain signal and resolution enhancement, Time-domain amplitude balancing and Frequency-domain low-frequency balancing.

From the raw volume data (Figure 1a), we can see that the S/N (signal to noise ratio) is quite low, especially in the study interval, and the exact fault positions can not be identified very confidently either. While the processed volume data show substantial improvement (Figure 1b). The continuities of fault traces are greatly improved since residual noises are attenuated further during above processing. Besides, more other details/features are also better revealed, such as the structures and even the termination patterns of seismic events. At the same time, from the Xline profile comparison in Figure 2, we can also see the improvement which further confirms the effectiveness of the adopted method.

Hosted by



Supported by



Chaired by



Co-chaired by



Conference Organisers



Event Organisers



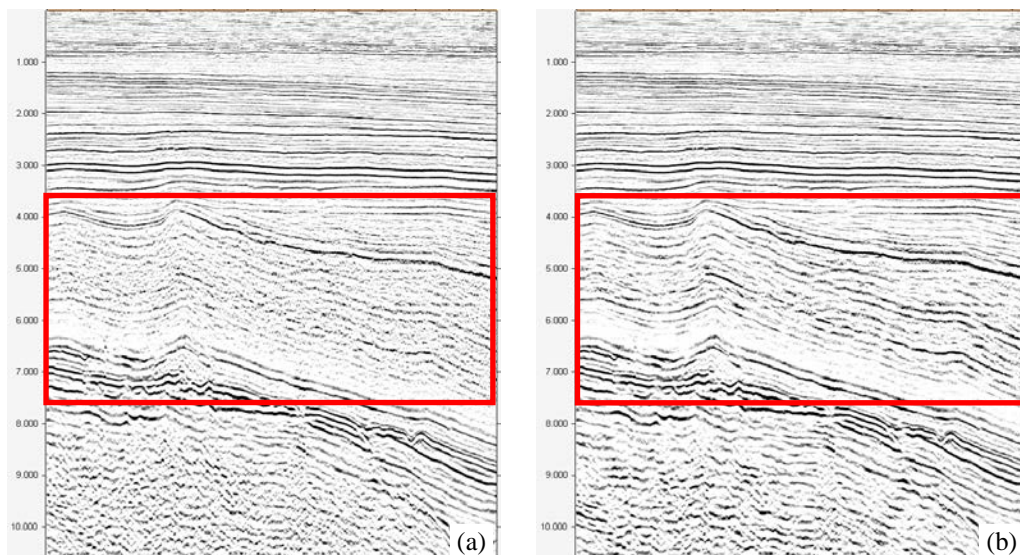


Figure 1. Seismic profile comparison (Inline) before and after “vector high fidelity signal enhance”; (a) before processing, (b) after processing; the red rectangle is round the study interval

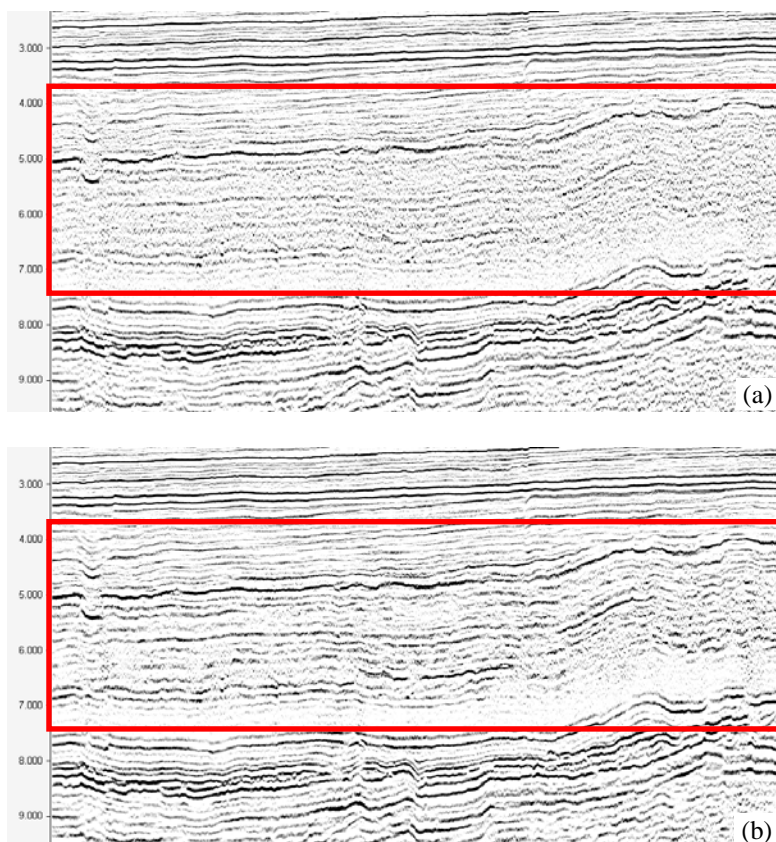


Figure 2. Seismic profile comparison (Xline) before and after “vector high fidelity signal enhance”; (a) before processing, (b) after processing; the red rectangle is round the study interval

The second step was to employ the technology of an “end-to-end convolutional neural network (CNN)” to efficiently detect faults from 3D seismic images. In this machine learning method, the fault detection was considered as a binary segmentation problem of labeling a 3D seismic image with ones on faults and zeros elsewhere, different from the conventional methods considering faults as seismic reflection discontinuities which were not very applicable and effective in the study area.

The workflow in this step: (1) Prepare Data. Firstly, vertical range cropping of input seismic cube is performed to narrow it down around the study interval, in order to learn more related information from study interval and to reduce potential computing time later; then structural smoothing is calculated upon input seismic cube to further denoise it; at last labeling a small set of faults in the cube with expert experiences used for subsequent machine learning training, and very clean fault labeling is preferred here by avoiding incomplete, duplicated and mismatched interpretations to seismic signal. (2) Build Training Dataset. U-Net image segmentation deep learning CNN framework is chosen, which requires that the input and output are both images with the same size. Therefore, each full seismic amplitude profile and related fault interpretations are split into a series of single training sample pairs with 512×512 pixels. At last, the training dataset contains 7222 pairs from interpreted Inline, Xline and random line profiles. (3) Design Deep Learning Network (U-Net). This deep neural network is implemented with Keras functional API. Output from the network is a 512×512 pixel image which represents mask (fault interpretation) that should be learned. Sigmoid activation function makes sure that mask pixels are in [0, 1] range. This U-Net framework contains the operations of Convolution, Copy and crop, Max pool, and Up-convolution. (4) Train U-Net Model. The model is trained for 3 epochs. After 3 epochs, the calculated accuracy is about 0.9775. Loss function for the training is basically a binary cross-entropy. The training process is based on a winserver2016 with Intel Xeon Gold 6246 CPU 3.30 GHz (2 processors), 192 GB Memory and Nvidia 8G GPU. Total training time is very short and less than 30 minutes on this machine.

To verify the performance of the above machine learning, a seismic profile in another direction is used (Figure 3). This figure compares the fault prediction results from conventional edge-detection variance attribute, opensource pre-trained model, re-trained model in this paper, and expert’s interpretation. It shows that the re-trained U-Net model in this paper have following unique advantages: the fault prediction result is more like manually interpreted faults; can generate clean/clear fault predictions with still sort of noisy seismic data; can successfully identify Y-shape fault pattern; can identify new faults accurately beyond expert’s experiences.

The third step was to make “auto fault patch extraction” and then coalesced them with some manual work to make sure they conformed to certain structural patterns according to the regional geological knowledge (Figure 4).



The fault system was revealed much more clearly than the old ones. Controlled by multi-stage regional stress fields, multiple sets of NW, NE, and rough EW-trending faults developed in study interval, showing complex tectonic deformation characteristics in which thrust faults and strike-slip faults interweaved. More importantly, the new fault system had more obvious control on karsted carbonate reservoir development and even hydrocarbon accumulation. The deep and large faults cutting into the Cambrian were not only effective channels for upward migration of oil and gas, but also effective enhancer for the storage performance of otherwise low-porosity and low-permeability carbonate reservoirs. A diagrammatic fault-controlled carbonate reservoir development model was proposed based on the new fault system interpretation and its controls on oil and gas accumulations with real E&P data evidence (Figure 5).

It is the first time to apply these advanced technologies for fault system mapping in the study area and obtain much better results that can be used directly for better E&P activities, and this can also be used as reference for similar industrial projects.

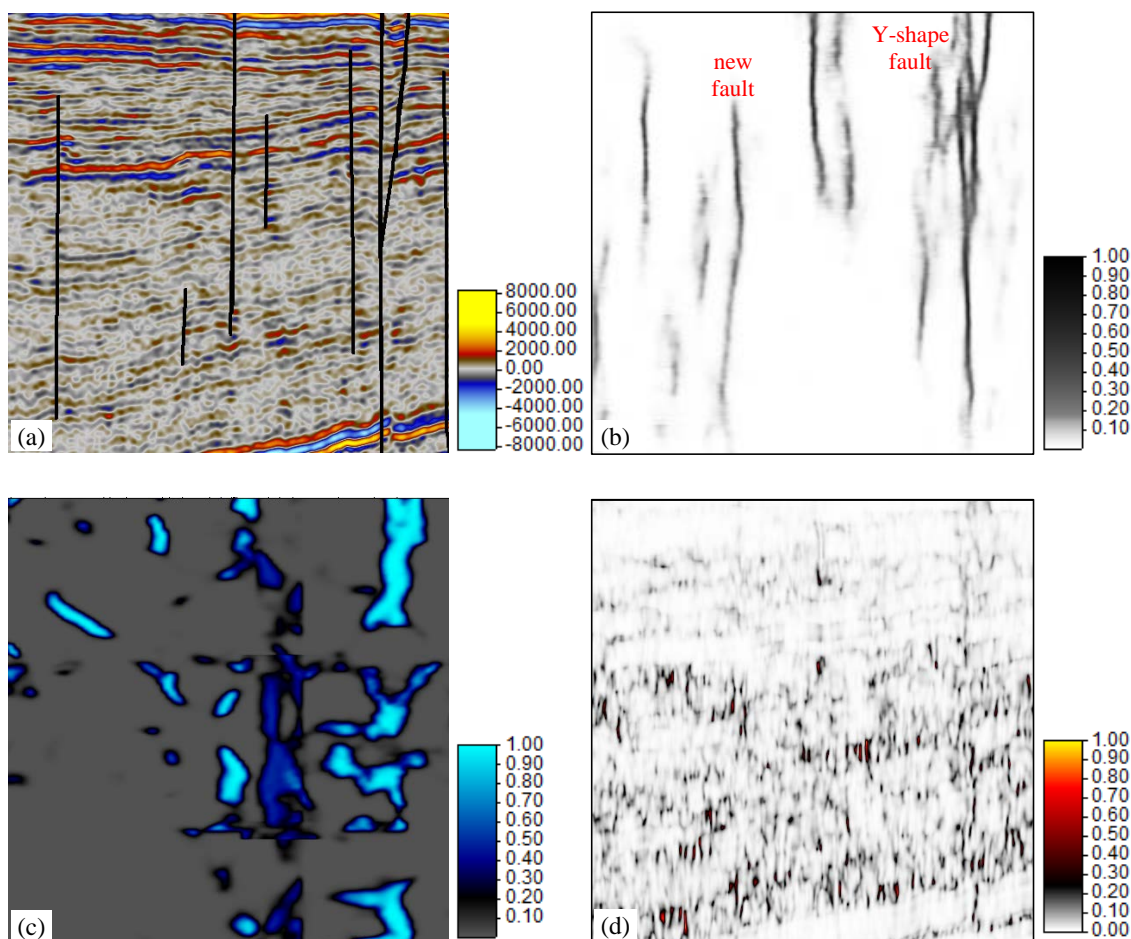


Figure 3. Fault comparison on the same seismic profile; (a) expert's interpretation, (b) prediction with the re-trained model in this paper, (c) prediction with a pre-trained model, and (d) conventional edge-detection variance attribute

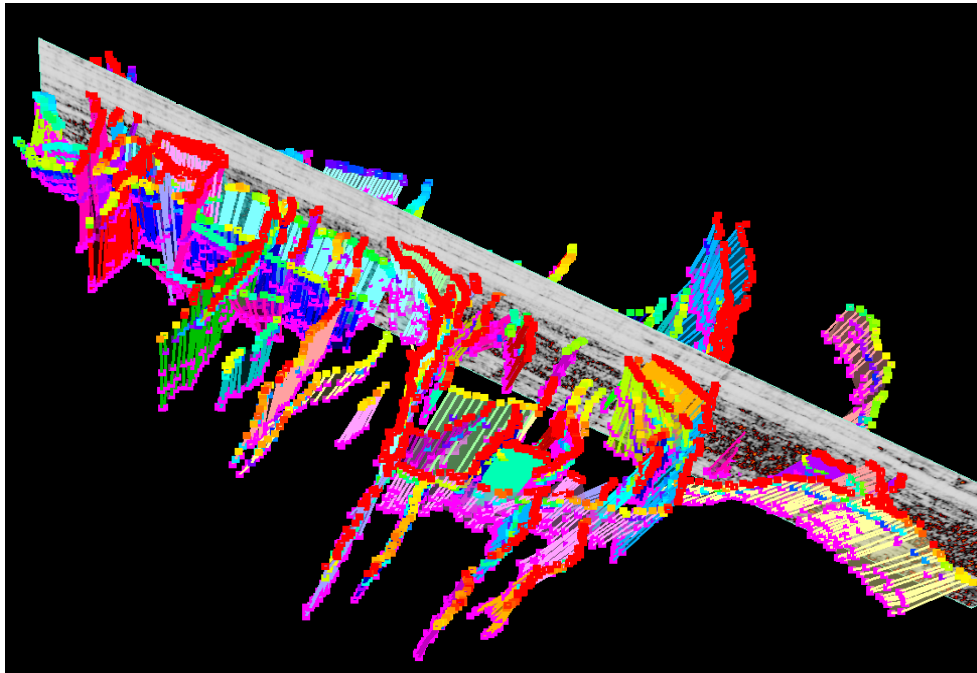


Figure 4. Final fault interpretations displayed in 3D window

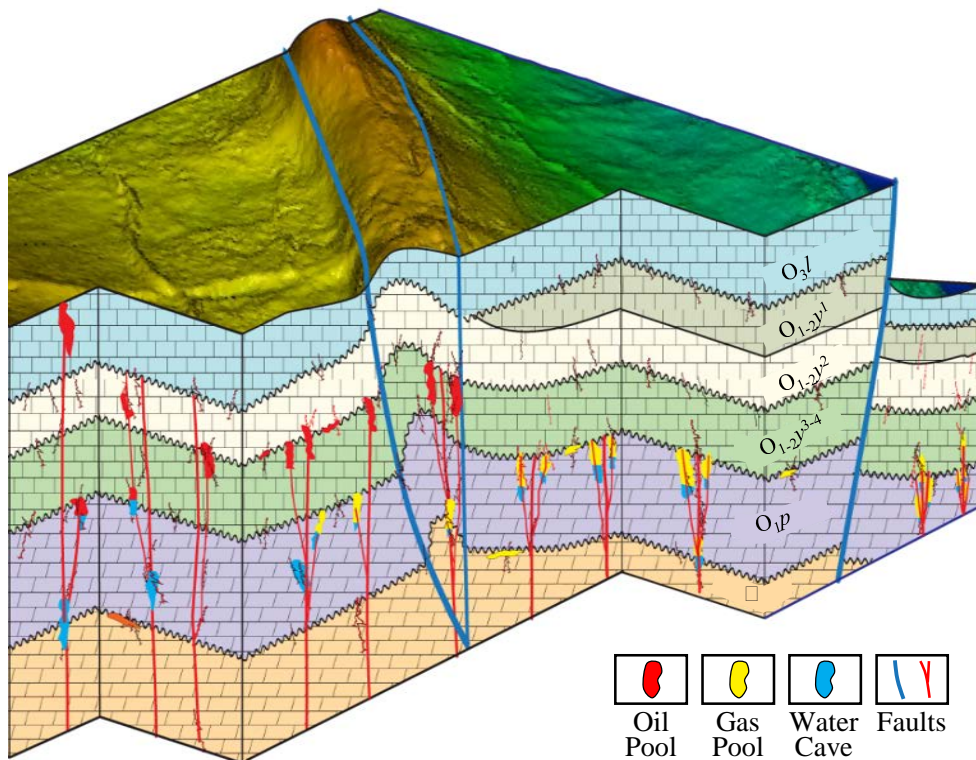


Figure 5. Diagrammatic model showing the composite oil and gas accumulations in study area

### References

- [1] S. Spitz, 1991. Seismic trace interpolation in the F-X domain. *GEOPHYSICS*, 56(6): 785-794
- [2] G. Beylkin, 1987. Discrete radon transform. *IEEE transactions on acoustics, speech, and signal processing*, ASSP-35(2): 162-172
- [3] X. Wu, L. Liang, Y. Shi, *et al*, 2019. FaultSeg3D: Using synthetic data sets to train an end-to-end convolutional neural network for 3D seismic fault segmentation. *GEOPHYSICS*, 84(3): IM35-IM45